

# Rab1 recruits WHAMM during membrane remodeling but limits actin nucleation

Ashley J. Russo<sup>a</sup>, Alyssa J. Mathiowetz<sup>a</sup>, Steven Hong<sup>a</sup>, Matthew D. Welch<sup>b</sup>, and Kenneth G. Campellone<sup>a,\*</sup>

<sup>a</sup>Department of Molecular and Cell Biology, Institute for Systems Genomics, University of Connecticut, Storrs, CT 06269; <sup>b</sup>Department of Molecular and Cell Biology, University of California, Berkeley, Berkeley, CA 94720

**ABSTRACT** Small G-proteins are key regulatory molecules that activate the actin nucleation machinery to drive cytoskeletal rearrangements during plasma membrane remodeling. However, the ability of small G-proteins to interact with nucleation factors on internal membranes to control trafficking processes has not been well characterized. Here we investigated roles for members of the Rho, Arf, and Rab G-protein families in regulating WASP homologue associated with actin, membranes, and microtubules (WHAMM), an activator of Arp2/3 complex-mediated actin nucleation. We found that Rab1 stimulated the formation and elongation of WHAMM-associated membrane tubules in cells. Active Rab1 recruited WHAMM to dynamic tubulovesicular structures in fibroblasts, and an active prenylated version of Rab1 bound directly to an N-terminal domain of WHAMM *in vitro*. In contrast to other G-protein-nucleation factor interactions, Rab1 binding inhibited WHAMM-mediated actin assembly. This ability of Rab1 to regulate WHAMM and the Arp2/3 complex represents a distinct strategy for membrane remodeling in which a Rab G-protein recruits the actin nucleation machinery but dampens its activity.

**Monitoring Editor**  
Laurent Blanchoin  
CEA Grenoble

Received: Jul 16, 2015  
Revised: Jan 11, 2016  
Accepted: Jan 20, 2016

## INTRODUCTION

The actin cytoskeleton is crucial for establishing, maintaining, and changing the shape of mammalian cells (Pollard and Cooper, 2009). However, compared with recognized roles for actin rearrangements in remodeling the plasma membrane, relatively little is known about how the actin nucleation machinery influences the shape or movement of the organelles that comprise the secretory system. For example, the endoplasmic reticulum (ER), Golgi apparatus, and ER–Golgi intermediate compartment (ERGIC) have distinct morphologies tailored to their functions, but each is also reorganized

into pleiomorphic carriers that transport cargo. The regulation and function of the actin cytoskeleton in these remodeling processes are not well understood.

Branched actin filament networks are assembled by a heptameric macromolecule called the Arp2/3 complex and nucleation-promoting factors from the Wiskott–Aldrich syndrome protein (WASP) family, which direct Arp2/3-mediated actin polymerization during different cellular processes. Among the ubiquitously expressed factors, N-WASP facilitates receptor-mediated endocytosis and actin-based vesicle motility, WASH controls endosome shape and trafficking, and WAVE1, WAVE2, and WAVE3 drive protrusions of the plasma membrane during cell migration (Campellone and Welch, 2010; Rotty *et al.*, 2013; Seaman *et al.*, 2013). Junction-mediating and regulatory protein (JMY) is a WASP-family member with multiple cellular activities, such as increasing cell motility, facilitating transport from the *trans*-Golgi to the plasma membrane, and enhancing autophagosome biogenesis (Coutts *et al.*, 2009, 2015; Zuchero *et al.*, 2009; Schluter *et al.*, 2014). WHAMM shares 33% sequence identity with JMY and also functions in remodeling membranes of the conventional secretory pathway, but WHAMM primarily acts between the ER and Golgi (Campellone *et al.*, 2008). WHAMM can additionally drive the actin-based “rocketing” motility

This article was published online ahead of print in MBoc in Press (<http://www.molbiolcell.org/cgi/doi/10.1091/mbc.E15-07-0508>) on January 28, 2016.

\*Address correspondence to: Kenneth G. Campellone ([kenneth.campellone@uconn.edu](mailto:kenneth.campellone@uconn.edu)).

Abbreviations used: CC, coiled-coil; JMY, junction mediating and regulatory; PWCA, polyproline WASP-homology-2 connector acidic; WASP, Wiskott–Aldrich syndrome protein; WHAMM, WASP homologue associated with actin membranes and microtubules; WMD, WHAMM membrane-interaction domain.

© 2016 Russo *et al.* This article is distributed by The American Society for Cell Biology under license from the author(s). Two months after publication it is available to the public under an Attribution–Noncommercial–Share Alike 3.0 Unported Creative Commons License (<http://creativecommons.org/licenses/by-nc-sa/3.0>).

“ASCB®,” “The American Society for Cell Biology®,” and “Molecular Biology of the Cell®” are registered trademarks of The American Society for Cell Biology.

of autophagosomes that arise from subdomains of the ER (Kast *et al.*, 2015).

Endogenous WHAMM localizes to the *cis*-Golgi and dynamic tubulovesicular ERGIC-like structures (Campellone *et al.*, 2008). Consistent with a role in organizing and trafficking secretory membranes, depletion of WHAMM causes a dispersion of the Golgi away from the microtubule-organizing center and delays transport of the viral glycoprotein VSV-G from the ER to the Golgi and cell surface (Campellone *et al.*, 2008). In contrast, slightly elevating WHAMM protein levels increases the appearance of tubular membranes that move in an actin- and/or microtubule-dependent manner (Campellone *et al.*, 2008). Simultaneous binding of WHAMM to liposomes and microtubules *in vitro* promotes an initial deformation of membranes (Shen *et al.*, 2012), whereas actin nucleation via WHAMM and Arp2/3 complex in cells can drive the elongation of membrane tubules (Campellone *et al.*, 2008). However, the regulatory factors that govern these processes are not known.

Studies on the regulation of WASP-family proteins indicate that their localization and activity are often controlled by the Rho family of small G-proteins. For example, N-WASP and WAVE1/WAVE2 can be recruited to the plasma membrane and activated by Cdc42 and Rac1 (Miki *et al.*, 1998a,b; Rohatgi *et al.*, 1999; Eden *et al.*, 2002; Steffen *et al.*, 2004; Innocenti *et al.*, 2005). Cdc42 has also been implicated in Golgi to ER transport, perhaps acting upstream of N-WASP (Luna *et al.*, 2002; Matas *et al.*, 2004), and full activation of WAVE2 requires costimulation by a second G-protein, membrane-associated Arf1 (Koronakis *et al.*, 2011). However, altering the expression of N-WASP, WAVE1, or WAVE2 does not substantially affect the organization of the ER or Golgi (Campellone *et al.*, 2008). Of interest, the atypical Rho-family member RhoD (Aspenstrom, 2014) interacts with WHAMM in cell extracts (Gad *et al.*, 2012) and influences Golgi-related transport (Blom *et al.*, 2015), but it is not clear whether their interaction affects membrane remodeling or actin nucleation.

Multiple small G-proteins, especially several from the Sar/Arf and Rab families, control the organization and trafficking of ER and Golgi membranes (Gillingham and Munro, 2007; Hehnlly and Stamnes, 2007; Kahn, 2009; Saraste *et al.*, 2009; Zanetti *et al.*, 2011; Egea *et al.*, 2013) and are therefore good candidates for regulating cytoskeletal rearrangements at these organelles. In humans, this includes two Sar1 isoforms (Sar1a and Sar1b), which control COPII vesicle coat assembly and ER exit, and Arf1, which controls COPI coat assembly on ERGIC and Golgi membranes. In addition, two Rab1 isoforms (Rab1a and Rab1b), which are 92% identical, function in several aspects of ER–Golgi transport, including vesicle tethering (Plutner *et al.*, 1991; Tisdale *et al.*, 1992; Pind *et al.*, 1994; Allan *et al.*, 2000; Moyer *et al.*, 2001). Rab1 proteins also associate with ERGIC membranes, where they influence Golgi-directed and perhaps unconventional Golgi-independent carriers (Sannerud *et al.*, 2006; Marie *et al.*, 2009).

The established roles for small GTPases in recruiting and activating nucleation factors led us to explore whether several G-proteins that are known to operate in the secretory pathway might influence WHAMM-mediated membrane remodeling. Our results uncover a new mechanism of dialogue between Rab-family G-proteins and the actin nucleation machinery and highlight a role for Rab1 in limiting WHAMM-associated actin assembly.

## RESULTS

### Rab1 stimulates tubulation of WHAMM-associated membranes

WHAMM promotes membrane tubulation, but the mechanisms that regulate this process are not well understood. To test whether small

G-proteins affect WHAMM-mediated membrane tubulation, we transiently coexpressed mCherry-tagged WHAMM with green fluorescent protein (GFP)-tagged versions of Sar1a, Rab1a, Arf1, Cdc42, or RhoD in fibroblasts and quantified the fraction of cells with membrane tubules, defined as WHAMM-associated structures that were  $>1 \mu\text{m}$  long and not within the Golgi. As shown previously (Campellone *et al.*, 2008), mCherry-WHAMM localized to the Golgi region and to tubulovesicular structures in the cell periphery (Figure 1A). Approximately 12% of cells expressing mCherry-WHAMM alone or in combination with GFP contained membrane tubules that typically measured several micrometers in length (Figure 1B). Coexpression of WHAMM with Sar1a, Arf1, Cdc42, or RhoD did not affect the fraction of cells with visible membrane tubules (Figure 1B). However, coexpression of mCherry-WHAMM with GFP-Rab1a increased the fraction of cells with tubules to 80% (Figure 1, A and B). We observed similar results after exchanging the fluorescence tags on WHAMM and Rab1, as  $>80\%$  of cotransfected cells harbored tubules, compared with 10–15% of cells expressing GFP-WHAMM alone (Supplemental Figure S1A). When expressed by itself, mCherry-Rab1a also showed a tubular localization pattern in 10–15% of cells (Supplemental Figure S1A), implying that these structures are the same as those induced by WHAMM (later discussion of Figure 2). Of interest, when examining cells coexpressing fluorescent WHAMM and Rab1a, we noticed that many tubules were unusually long ( $>5 \mu\text{m}$ ) and even branched (Figure 1A). Whereas  $<5\%$  of cells coexpressing mCherry-WHAMM with Sar1a, Arf1, Cdc42, or RhoD contained tubules  $>5 \mu\text{m}$  long,  $>50\%$  of cells coexpressing mCherry-WHAMM and GFP-Rab1a harbored such long tubules (Figure 1B). Thus, among our set of canonical ER- and Golgi-associated G-proteins, Rab1 possesses the specific ability to increase the number and length of WHAMM-associated membrane tubules.

To determine whether the nucleotide-binding state of Rab1 influences these membrane remodeling events, we coexpressed GFP-WHAMM with a constitutively active GTP-bound mutant (Q70L) of Rab1a or two inactive versions of Rab1a, one (S25N) locked in a GDP-bound state and another (N124I) defective in nucleotide binding (Tisdale *et al.*, 1992). Cells expressing the active Rab1a mutant formed WHAMM-associated tubules as frequently as those expressing the wild-type version (Figure 1C), indicating that GTP-bound Rab1 can stimulate tubulation. In contrast, the two inactive Rab1a mutants behaved as dominant-negative inhibitors of membrane tubulation. Compared to the basal level of tubulation in cells expressing the mCherry vector, threefold-to-fourfold fewer cells expressing the mCherry-tagged S25N or N124I variants contained WHAMM tubules (Figure 1C), suggesting that Rab1 activation is crucial for tubule biogenesis.

To further test whether Rab1 is important for membrane tubulation, we targeted Rab1a and Rab1b for silencing using small interfering RNAs (siRNAs) and assessed the effect on GFP-WHAMM-associated membrane remodeling. Immunoblotting and immunostaining of transfected cells with polyclonal Rab1 antibodies indicated that, aside from a weak nuclear staining pattern, Rab1 protein levels were nearly abolished in response to three independent pairs of Rab1a+b siRNAs (Supplemental Figure S1, B and C). Of interest, Rab1 depletion was associated with a twofold-to-fivefold reduction in the fraction of GFP-WHAMM-expressing cells containing membrane tubules (Figure 1C). We also treated cells with siRNAs to RhoD (Supplemental Figure S1B), but RhoD targeting did not significantly affect tubulation driven by GFP-WHAMM (Figure 1C) or by coexpression of GFP-WHAMM with mCherry-Rab1 (Supplemental Figure S1D). Taken together, our dominant-negative and depletion studies

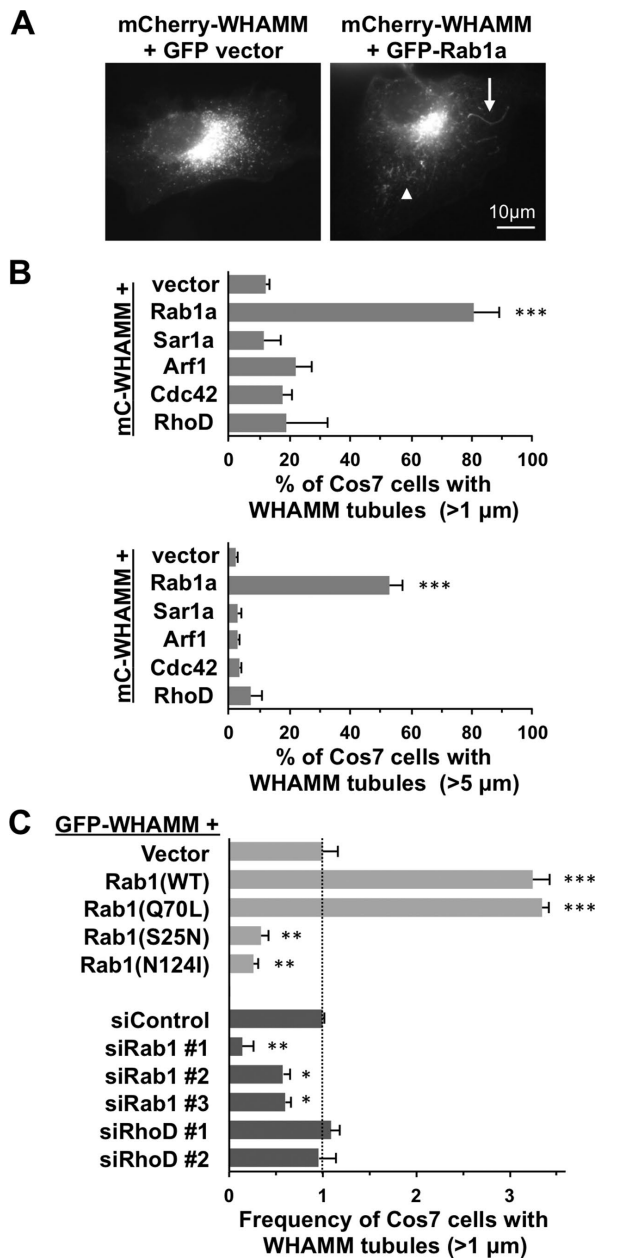


**FIGURE 1:** Rab1 stimulates tubulation of WHAMM-associated membranes. (A) Cos7 cells were transfected with plasmids encoding mCherry-WHAMM and GFP or GFP-Rab1a, fixed, and examined by fluorescence microscopy. Arrowhead and arrow highlight examples of short (1–5 μm) and long (>5 μm) membrane tubules, respectively. (B) Cos7 cells were cotransfected with plasmids encoding mCherry-WHAMM and GFP-tagged versions of Rab1a, Sar1a, Arf1, Cdc42, or RhoD. The percentage of cells with WHAMM-associated structures >1 μm or >5 μm in length was quantified. (C) Cos7 cells were cotransfected with plasmids encoding GFP-WHAMM and mCherry-tagged versions of wild-type (WT) Rab1a, constitutively active (CA) Rab1a (Q70L), or dominant-negative (DN) inactive Rab1a (S25N or N124I). Alternatively, Cos7 cells were cotransfected with a plasmid encoding GFP-WHAMM and a control siRNA, siRNAs to Rab1a and Rab1b, or siRNAs to RhoD. The percentage of cells with WHAMM-associated structures >1 μm in length was quantified, and cells expressing the mCherry vector or transfected with control siRNAs were each set to 1 for normalization. In B and C, every bar represents the mean ± SD from three to five experiments in which 50–100 cells were counted per experiment. \*\*\* $p < 0.001$ , \*\* $p < 0.01$ , \* $p < 0.05$ ; ANOVA with Dunnett's posttest. See Supplemental Figure S1.

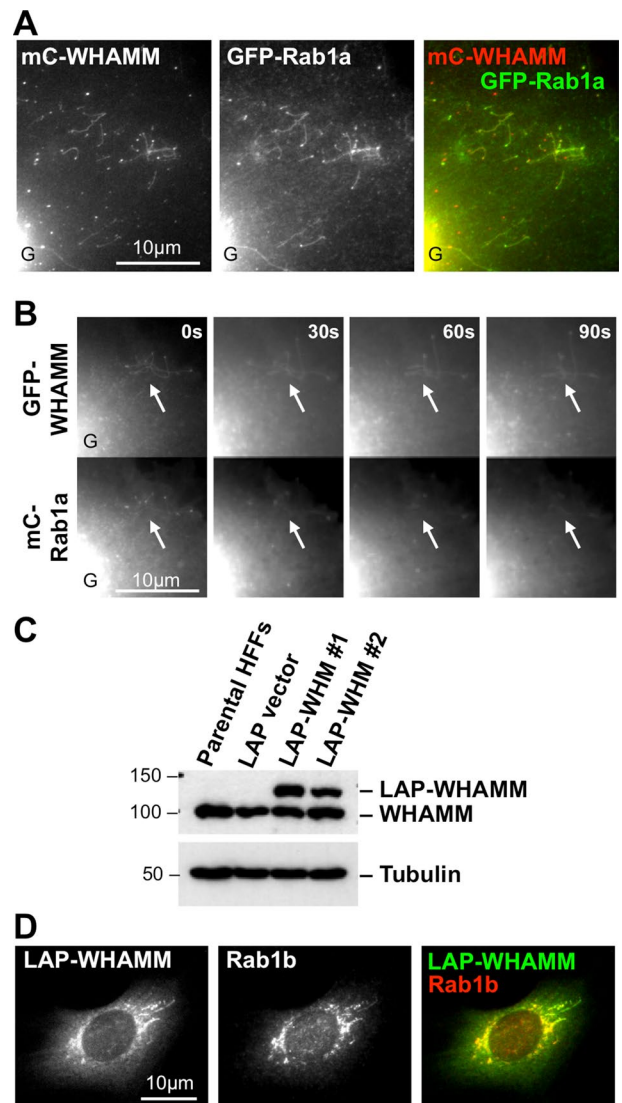


**FIGURE 2:** WHAMM and Rab1 colocalize at the Golgi region and along dynamic tubulovesicular membranes. (A) Cos7 cells were cotransfected with plasmids encoding mCherry-WHAMM and GFP-Rab1a (WT) and fixed. Colocalization along tubulovesicular structures at the periphery of a cell is shown. The edge of the intensely fluorescent Golgi region is indicated G. (B) Cos7 cells were cotransfected with GFP-WHAMM and mCherry-Rab1a plasmids (WT) and examined live. Arrows highlight areas of active tubule dynamics (Supplemental Video S1). (C) HFF clones stably expressing the LAP tag or LAP-WHAMM (WHM) were lysed and subjected to immunoblotting with antibodies to WHAMM or tubulin. (D) HFFs stably expressing LAP-WHAMM were fixed and stained with polyclonal antibodies to Rab1b. See Supplemental Figure S2.

highlight a specific functional relationship between active Rab1 and the remodeling of WHAMM-associated membranes.

### WHAMM and Rab1 colocalize at the Golgi and ER-associated tubular membranes

Given that Rab1 has a major influence on the ability of WHAMM to promote membrane tubulation, we next examined the localization of Rab1 during this process. Like WHAMM, Rab1 is found at the *cis*-Golgi and ERGIC (Plutner *et al.*, 1991; Sannerud *et al.*, 2006), so it was not surprising that we visualized a prominent juxtannuclear localization for GFP-Rab1a (e.g., Figure 2, A and B, lower left). Strikingly,

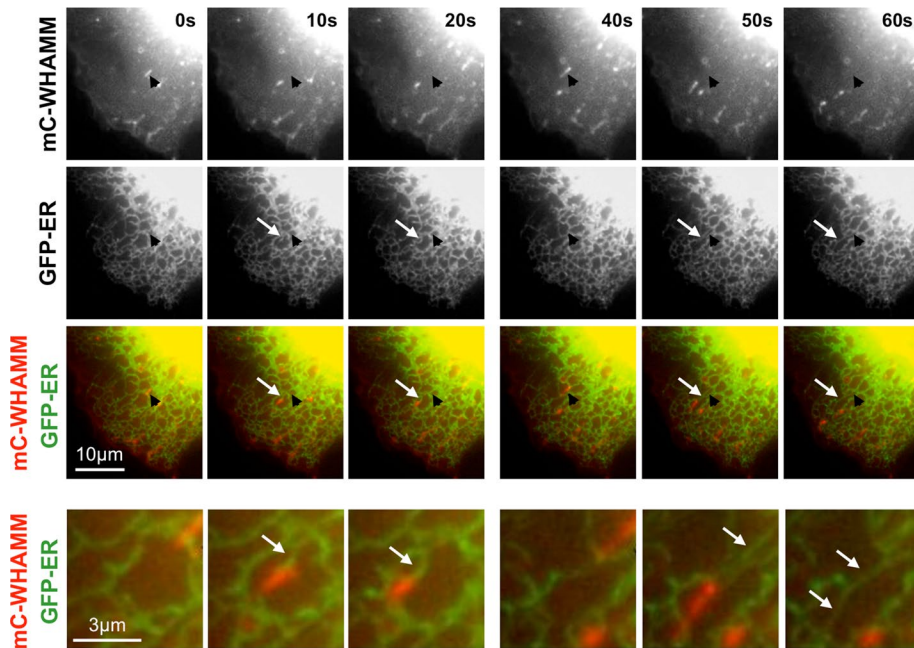


**FIGURE 3:** WHAMM-associated tubules are connected to the ER. Cos7 cells were cotransfected with plasmids encoding mCherry-WHAMM and GFP-ER (a calreticulin signal sequence followed by GFP and a KDEL retrieval sequence) and examined live. Black arrowheads indicate the starting position of a WHAMM-associated tubule, and white arrows highlight areas where tubule movement is trailed by ER membrane. The bottom row shows a higher magnification of the region of interest. See Supplemental Videos S2 and S3.

however, GFP-Rab1a was also found on the WHAMM-associated tubulovesicular membranes in the periphery of cotransfected cells (Figure 2A). Although cells harbored some independent Rab1- and WHAMM-associated vesicles, mCherry-WHAMM and GFP-Rab1a exhibited nearly perfect colocalization along virtually every tubulovesicular structure (Figure 2A).

Tagged WHAMM has been reported to overlap with RhoD in the Golgi region (Blom *et al.*, 2015), so we also assessed the position of various fluorescent forms of WHAMM and RhoD. In contrast to mCherry-Rab1, which was found at the Golgi and/or tubulovesicular membranes in >90% of cells, mCherry-RhoD was found in the cytosol and at the plasma membrane in most cells, although ~30% of cells included some juxtannuclear Golgi-like localization (Supplemental Figure S2, A and B). When we expressed WHAMM to induce membrane tubulation, RhoD was not detected along the WHAMM-associated tubulovesicular structures (Supplemental Figure S2, B and C). Thus, whereas WHAMM, Rab1, and RhoD can all be found at the Golgi to some degree, Rab1 is the specific G-protein that colocalizes with WHAMM on tubulovesicular membranes.

To further characterize the colocalization of Rab1 and WHAMM, we visualized tubule dynamics in live cells. Of interest, mCherry-Rab1a mirrored the localization of GFP-WHAMM along tubular membranes whether they were stationary, elongating, branching, or shrinking (Figure 2B and Supplemental Video S1). These results support the idea that Rab1 cooperates with WHAMM during multiple aspects of the tubulation process.

To confirm the colocalization of Rab1 and WHAMM, we sought to compare the location of the endogenous molecules. However, the fixation conditions for WHAMM and Rab1 antibody staining were incompatible (see *Materials and Methods*). Therefore we generated cell lines that stably express a localization and affinity purification (LAP; Cheeseman and Desai, 2005)-tagged WHAMM variant

with a histidine (His)-GFP tag at its N-terminus (Campellone *et al.*, 2008). We isolated two human foreskin fibroblast (HFF) clones expressing LAP-WHAMM at a level similar to that of endogenous WHAMM (Figure 2C) and then fixed and stained the cells with polyclonal Rab1b antibodies. Endogenous Rab1 colocalized with LAP-WHAMM at the Golgi region and along tubular structures (Figure 2D). Thus the localization of both tagged and endogenous Rab1 is consistent with a direct role in WHAMM-mediated membrane tubulation.

We next attempted to better characterize the identity of the tubulovesicular membranes. Because Rab1 and WHAMM both influence ER-to-Golgi transport (Hutagalung and Novick, 2011; Mizuno-Yamasaki *et al.*, 2012; Campellone *et al.*, 2008), we examined the movement of mCherry-WHAMM-associated membranes in live cells coexpressing GFP in the ER lumen. WHAMM-associated vesicles found in the periphery of the cell were frequently moving but always appeared to be tethered to the ER (Supplemental Video S2). Similarly, short WHAMM-associated tubules were also connected to the ER (Figure 3). Of interest, as the short WHAMM tubules traveled toward the cell periphery, they often appeared to be trailed by ER

membrane (Figure 3 and Supplemental Video S3). Thus at least some of the WHAMM-associated tubulovesicular membranes are involved in ER network remodeling.

### Rab1 is important for the association of WHAMM with organelle membranes

Because Rab1 enables the recruitment of its effector proteins to membranes (Allan *et al.*, 2000; Brandon *et al.*, 2006), we hypothesized that a key function of Rab1 in tubulation is to recruit WHAMM to membranes. To test this, we examined the localization of GFP-WHAMM more closely in cells coexpressing the mCherry-Rab1 derivatives. As described earlier (Figure 1), when the wild-type or active Q70L mutant of Rab1a was expressed, GFP-WHAMM displayed a Golgi and tubulovesicular localization (Figure 4A). However, when either the S25N or N124I mutant was expressed, not only did the cells fail to assemble tubules, but in addition GFP-WHAMM exhibited a diffuse cytoplasmic localization (Figure 4A). These dominant-negative Rabs did not cause a global redistribution of Golgi-associated proteins into the cytosol, because the *cis*-Golgi peripheral membrane protein GM130 was still found on puncta that were more discrete and dispersed in S25N-expressing cells (Figure 4B) and in cells coexpressing S25N with GFP-WHAMM (Figure 4C). These results suggest that the inactive mutants act as inhibitors of membrane tubulation by causing relocalization of WHAMM from membranes to the cytosol.

To verify that Rab1 is important for recruitment of WHAMM to membranes, we examined the ability of endogenous WHAMM to cosediment with cell membranes in the presence or absence of Rab1. We treated cells with control siRNAs or siRNAs to deplete Rab1, generated cell extracts, fractionated them into their membrane and cytosolic components by centrifugation, and tested for the presence of WHAMM by immunoblotting. Under these conditions, WHAMM was

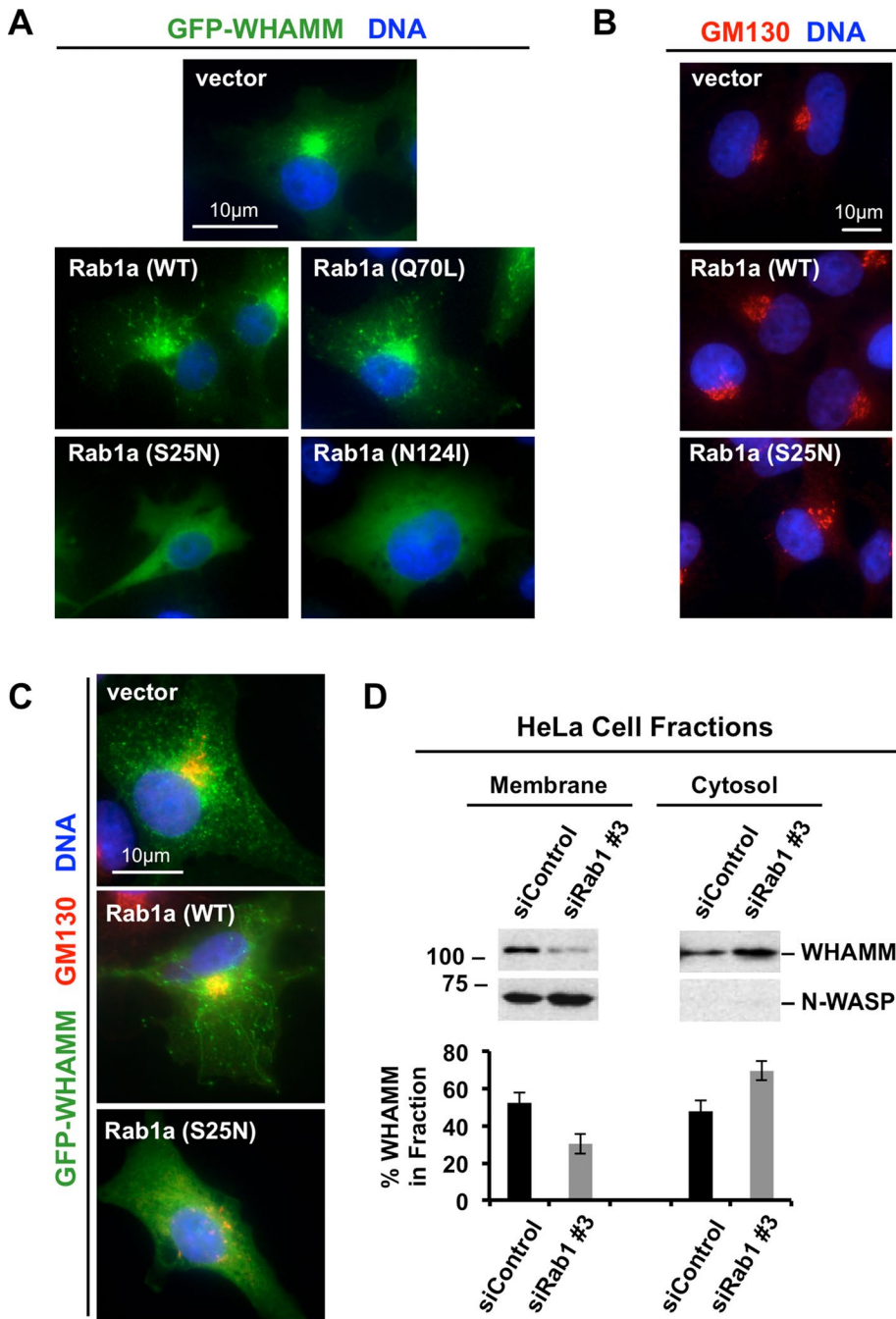


**FIGURE 4:** Rab1 is important for the association of WHAMM with organelle membranes. (A) Cos7 cells were cotransfected with plasmids encoding GFP-WHAMM and WT, active (Q70L), or dominant-negative inactive (S25N or N124I) mCherry-Rab1a and fixed. GFP fluorescence is shown in green, and DAPI-stained DNA is blue. (B) Cos7 cells transfected with mCherry-Rab1a variants were stained with antibodies to GM130. (C) Cos7 cells cotransfected as in A were stained with antibodies to GM130. (D) HeLa cells were transfected with a control siRNA or with siRNAs to Rab1a and Rab1b. Cell extracts were then fractionated into their membrane and cytosolic components and examined by blotting with antibodies to WHAMM or N-WASP. The percentage of WHAMM in each fraction was determined by densitometry. Each bar represents the mean  $\pm$  SD from three experiments.

distributed evenly in both fractions of control cells (Figure 4D). In contrast, when cells were depleted of Rab1, the amount of WHAMM in the cytosolic fraction was more than double that of WHAMM in the membrane fraction (Figure 4D). This redistribution was not observed for the control protein N-WASP, which remained enriched in the

membrane fraction whether Rab1 was present or not (Figure 4D). In conclusion, microscopy and fractionation studies each show that Rab1 is key for the association between WHAMM and cellular membranes.

### An active prenylated form of Rab1 binds to the WHAMM membrane-interaction domain of WHAMM

Given our functional and localization studies, we sought to determine whether the ability of Rab1 to stimulate WHAMM recruitment and membrane remodeling could be due to a physical interaction between the two proteins. First, we purified glutathione S-transferase (GST)-tagged Rab1a wild type, Q70L, and S25N from *Escherichia coli* (Supplemental Figure S3A), immobilized the proteins on glutathione beads, and performed pull-down assays using fibroblast extracts. Anti-WHAMM immunoblotting of bead-associated proteins demonstrated that both the wild-type Rab1a and the GTP-locked Q70L mutant of Rab1a interacted with WHAMM, whereas the GDP-locked S25N mutant and GST did not (Figure 5A). Densitometry indicated that the Q70L variant pulled down slightly more WHAMM than wild-type Rab1, but neither one associated with N-WASP (Figure 5A). Thus active Rab1 is capable of efficiently interacting with WHAMM in cytoplasmic extracts.

The modular organization of WHAMM includes an N-terminal WHAMM membrane-interaction domain (WMD), a central coiled-coil (CC) portion that binds microtubules, and a C-terminal polyproline-WH2-connector-acidic (PWCA) region that drives actin nucleation (Figure 5B; Campellone *et al.*, 2008). To determine which part of WHAMM is responsible for the association with Rab1, we expressed each domain as a GFP-fusion protein in cells and generated extracts to use in pull-down assays with the purified GTP- or GDP-bound versions of GST-Rab1a. Of interest, we observed an interaction between the active Q70L mutant and the WMD (Figure 5C). These results are consistent with the previous observations that the WMD is sufficient for localizing to membranes in cells (Campellone *et al.*, 2008) and binding to crude liposomes *in vitro* (Shen *et al.*, 2012).

Each of the foregoing pull downs took place in cell extracts, so we could not distinguish whether WHAMM bound directly to Rab1 or other cytoplasmic factors mediated their interaction. To test for direct binding, we first purified maltose-binding protein (MBP)-tagged WHAMM and the WMD from baculovirus-infected Sf9 insect cells (Shen *et al.*, 2012). We also generated a recombinant prenylated form of Rab1 by expressing GST-Rab1a in insect cells and fractionating their cytoplasmic

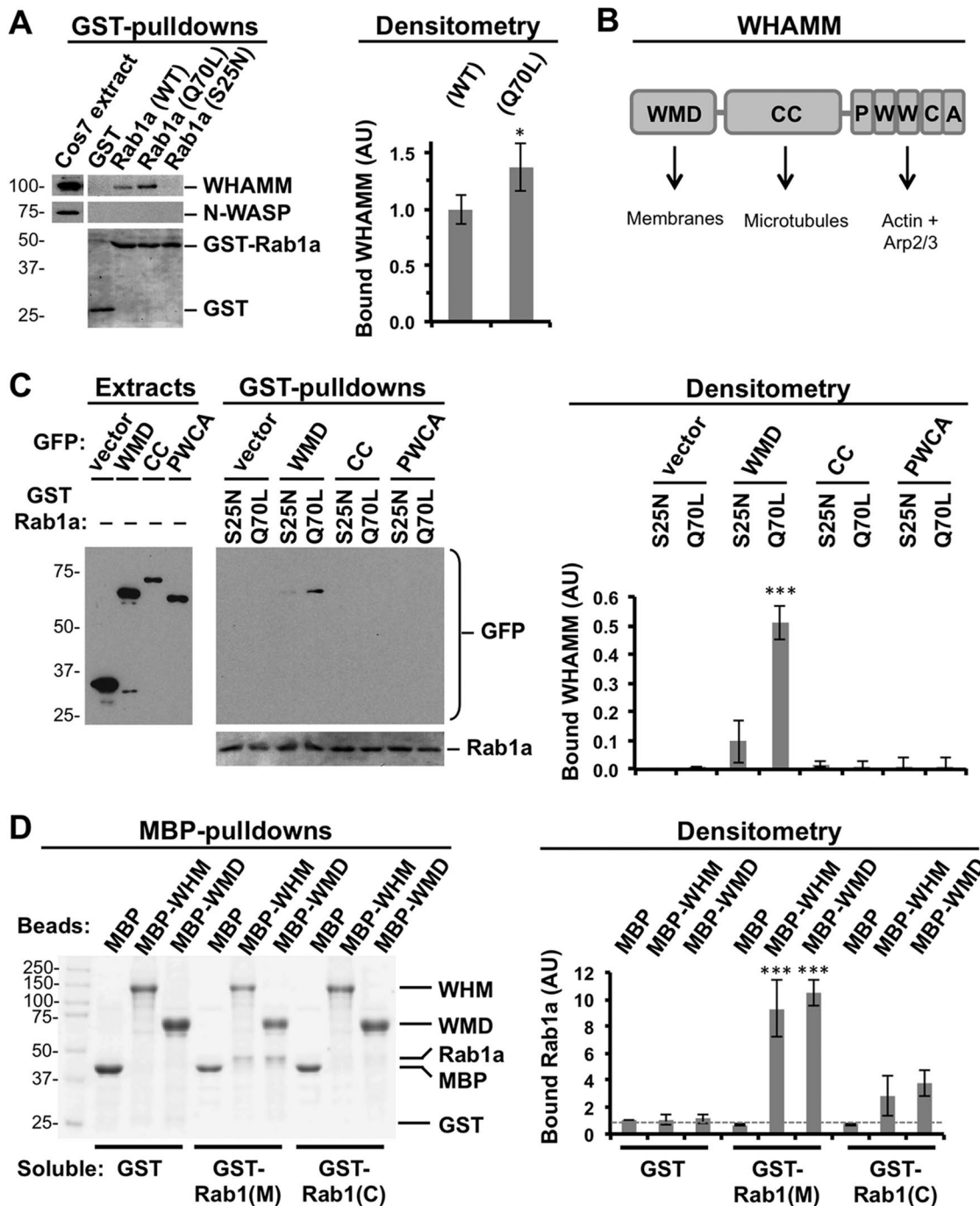


**FIGURE 5:** An active prenylated form of Rab1 binds to the WMD of WHAMM. (A) Purified GST or WT, active (Q70L), or inactive (S25N) GST-Rab1a were immobilized on beads and mixed with Cos7 cell extracts. Bead-associated proteins were subjected to SDS-PAGE and blotted with antibodies to WHAMM or N-WASP. GST and GST-Rab1a were visualized by Ponceau S staining. The relative amount of WHAMM that was pulled down was measured in arbitrary units (AU) by densitometry. (B) The modular domain organization of WHAMM includes an N-terminal WMD (residues 1–260) that localizes to membranes, a CC region (residues 261–630) that binds microtubules, and a C-terminal PWCA segment (residues 631–809) that engages actin and the Arp2/3 complex (Campellone and Welch, 2010). (C) Extracts from Cos7 cells transfected with plasmids encoding GFP or GFP-tagged WMD, CC, or PWCA were mixed with beads coated with active (Q70L) or inactive (S25N) GST-Rab1a. Bead-associated proteins were subjected to SDS-PAGE and blotted for GFP. GST-Rab1a was visualized with Ponceau S. The amount of WHAMM pulled down was determined by densitometry. (D) MBP or MBP-tagged full-length WHAMM (WHM) or the WMD were immobilized on beads and mixed with purified GST or GST-tagged versions of Rab1a that were membrane extracted (Rab1(M)) or cytosolic (Rab1(C)). Bead-associated proteins were subjected to SDS-PAGE and stained with Coomassie blue. The amount of GST proteins pulled down was determined by densitometry. In A–D, each bar represents the mean  $\pm$  SD from three experiments. \*\*\* $p < 0.001$ , ANOVA with Dunnett's posttest. \* $p < 0.05$ , with a paired  $t$  test. See Supplemental Figure S3.

components before purifying separate membrane-extracted (Rab1(M)) and cytosolic (Rab1(C)) forms of GST-Rab1a in the presence of excess GTP (Supplemental Figure S3B; Nuoffer *et al.*, 1995). In subsequent pull-down assays, MBP-WHAMM and MBP-WMD efficiently bound to Rab1(M) but showed little binding to Rab1(C) (Figure 5D). Neither WHAMM derivative bound to GST alone, and MBP did not interact with any of the GST-fusion proteins (Figure 5D), indicating that the physical interaction between the WMD and Rab1(M) was specific. Therefore we conclude that the WHAMM WMD binds directly to an active prenylated form of Rab1.

### Rab1 inhibits actin assembly in vitro

Because binding of other small G-proteins to WASP-family proteins can stimulate their actin nucleation-promoting activity (Miki *et al.*, 1998a,b; Rohatgi *et al.*, 1999; Eden *et al.*, 2002; Steffen *et al.*, 2004; Innocenti *et al.*, 2005), we next tested whether Rab1 might influence WHAMM-associated actin nucleation in vitro by examining actin assembly kinetics in fluorescent pyrene-actin polymerization assays. As expected based on previous results (Campellone *et al.*, 2008; Shen *et al.*, 2012), MBP-WHAMM and the Arp2/3 complex together accelerated actin assembly in this system of purified components (Figure 6A). Surprisingly, however, the addition of Rab1(M) caused a dose-dependent decrease in the rate of actin polymerization (Figure 6A). In contrast, a GST-RhoD derivative that was previously shown to pull down WHAMM from cell extracts (Gad *et al.*, 2012) did not inhibit actin assembly in the presence of purified full-length WHAMM (Figure 6B). The inhibitory effect of Rab1 was specific to the membrane-derived version of Rab1 and to WMD-containing constructs of WHAMM. In particular, Rab1(M) decreased the maximal actin polymerization rates when used at concentrations equimolar to or greater than full-length WHAMM (Figure 6C), whereas RhoD did not have any significant effect on actin assembly kinetics in the presence of high (200 nM) or low (50 nM) concentrations of WHAMM, even when present in a molar excess and loaded with GTP $\gamma$ S (Figure 6D). In contrast, Rab1(M) did not significantly slow actin assembly driven by the isolated PWCA domain from WHAMM (Figure 6, E and F) or the WCA domain from N-WASP (Figure 6G). Finally, G-proteins without an affinity for WHAMM, cytosolic Rab1(C) and membrane-extracted Rab5(M), did not affect the rate of actin polymerization in the presence of WHAMM or its PWCA segment (Figure 6C,F). Collectively these results indicate that Rab1(M) inhibits actin assembly driven by recombinant WHAMM and the Arp2/3 complex in vitro.

These findings were unexpected because WHAMM-mediated actin assembly was previously shown to promote the elongation of tubulovesicular membranes in cells (Campellone *et al.*, 2008). Indeed, similar to those previous observations, actin filaments were associated with the elongated membrane structures induced upon coexpression of WHAMM and Rab1 (Figure 7A and Supplemental Figure S4). However, when we examined these membranes at the resolution of individual tubulovesicular structures, we noticed that the actin filaments were predominantly found along the length of the tubule and were mostly absent from the vesicle head (Figure 7B). To quantify this, we measured the relative intensity of WHAMM, Rab1, and F-actin along tubulovesicular structures, setting the maximal intensity of WHAMM on the vesicle to 1. These analyses confirmed that the amounts of Rab1 and WHAMM both peaked in association with the vesicle, whereas F-actin intensity was low on the vesicle and consistently high along the length of the tubule (Figure 7C). Thus the ability of Rab1 to inhibit the actin nucleation-promoting function of WHAMM in vitro is consistent with an absence of actin filaments around the vesicle portions of tubulovesicular membranes in cells.

## DISCUSSION

The localization and activities of WASP-family nucleation factors have been known for many years to be controlled by small G-proteins. As the best-studied examples, active Cdc42 binds directly to WASP/N-WASP to relieve autoinhibition and promote localized actin assembly (Kim *et al.*, 2000; Prehoda *et al.*, 2000), whereas active Rac1 binds to the heteropentameric WAVE complex to stimulate WAVE1/WAVE2-mediated nucleation at plasma membrane protrusions (Chen *et al.*, 2010). Our results demonstrating the physical and functional interactions between Rab1 and WHAMM now reveal a new link between the ER-Golgi trafficking machinery and the actin nucleation machinery. They also add Rab1 to an emerging group of molecules that modulate Arp2/3 function, with other examples including Dip1/WISH/SPIN90, which directs Arp2/3 to generate unbranched filaments (Wagner *et al.*, 2013), and Arpin, which can inhibit Arp2/3-mediated nucleation and branching during cell migration (Dang *et al.*, 2013).

The interaction between WHAMM and Rab1 exhibits both similarities to and differences from how other WASP-family members are targeted by Rho-family GTPases. Like WASP and N-WASP, WHAMM is recruited to membranes by binding directly to its G-protein partner, although the preference for the prenylated G-protein form appears to be more pronounced for WHAMM with Rab1. The most significant and unexpected difference is that Rab1 inhibits actin assembly by WHAMM, whereas Rho GTPases stimulate actin assembly by other WASP-family proteins. Of interest, another WASP-family member, WASH, controls membrane remodeling and trafficking, but of endosomal membranes rather than secretory organelles or the plasma membrane (Seaman *et al.*, 2013). The role of G-proteins in regulating WASH functions are not known, so it will also be important to learn how WASH activity is turned on or off by small G-proteins. It seems likely that one or more Rab-family GTPases govern the recruitment and/or nucleation-promoting activity of WASH on its target endosomes.

Aside from Rab1, WHAMM was previously shown to interact with another small G-protein, RhoD (Gad *et al.*, 2012), which also plays a role in anterograde transport (Blom *et al.*, 2015). However, our results indicate that RhoD does not have any direct function in WHAMM-associated endomembrane tubulation in cells or in regulating the actin nucleation-promoting activity of purified WHAMM in vitro. Thus a direct link between WHAMM and RhoD in a specific membrane remodeling function has yet to be defined. Whether RhoD influences WHAMM activity in a distinct cellular process such as actin stress fiber assembly or disassembly (Gad *et al.*, 2012) remains to be determined.

Rab1 is a versatile G-protein that functions at multiple steps along the secretory pathway (Hutagalung and Novick, 2011; Mizuno-Yamasaki *et al.*, 2012). This includes ER budding (Tisdale *et al.*, 1992; Peter *et al.*, 1994), COPII coat dynamics (Slavin *et al.*, 2011), COPI coat recruitment (Alvarez *et al.*, 2003; Monetta *et al.*, 2007), ERGIC-associated trafficking (Pind *et al.*, 1994; Saraste *et al.*, 1995; Sannerud *et al.*, 2006; Marie *et al.*, 2009), and, finally, tethering and fusion at the *cis*-Golgi (Allan *et al.*, 2000; Moyer *et al.*, 2001; Satoh *et al.*, 2003). Our results now add another function for Rab1: regulating cytoskeleton-associated membrane remodeling. The tubulovesicular membranes that are remodeled by Rab1 and WHAMM appear to be related to organelles of the secretory pathway, as they are often connected to the ER (e.g., Figure 3) or Golgi (e.g., Figure 7). However, precisely how Rab1 promotes tubulation and how membrane scission takes place are not yet clear.

Previous work demonstrated that the ability of WHAMM to drive Arp2/3-mediated actin assembly is important for tubule elongation

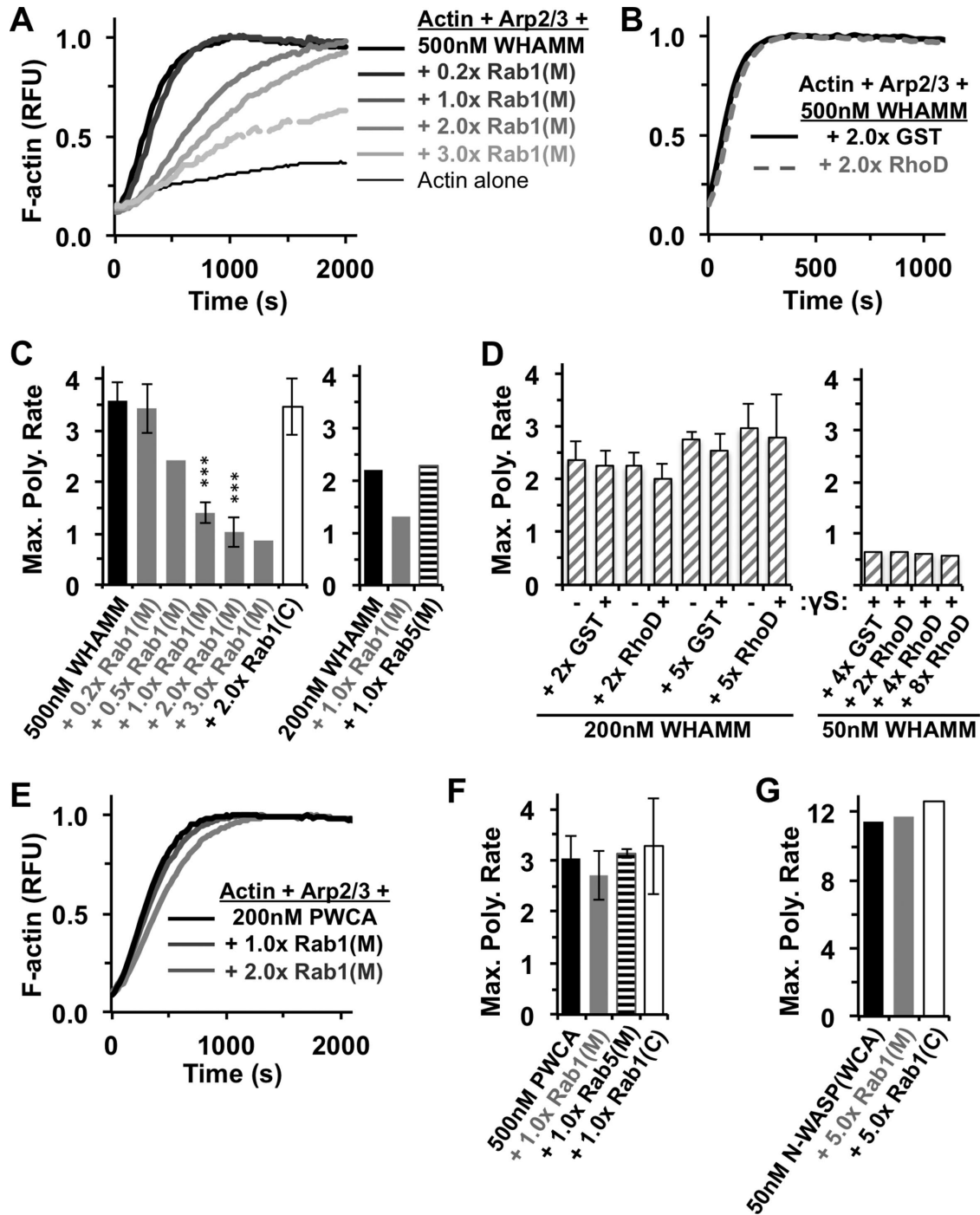


**FIGURE 6:** Rab1 inhibits actin assembly in vitro. Actin (2  $\mu$ M) was polymerized in the presence of 20 nM Arp2/3 complex, 50–500 nM MBP-WHAMM (full-length) or MBP-WHAMM (PWCA), or 50 nM His-N-WASP (WCA), with or without GST-Rab1(M), GST-Rab1(C), GST-RhoD, or GST-Rab5(M) derivatives. (A, B, E) Amount of F-actin, in relative fluorescence units (RFU), formed over time. (C, D, F, and G) Maximal actin assembly rates. The assembly rate for actin alone was  $\sim$ 0.12 nM/s. All data are from representative experiments, and error bars indicate the SDs from three or four experiments. \*\*\* $p < 0.001$ .

in cells (Campellone *et al.*, 2008), but our results indicate that Rab1 slows actin assembly in vitro. One possible explanation for these seemingly disparate findings is that after Rab1 recruits WHAMM to membranes, other, yet-to-be-defined factors activate WHAMM and the Arp2/3 complex to nucleate actin and promote membrane tubule elongation. The rate of actin polymerization, however, would be limited by the inhibitory activity of Rab1. Moreover, based on the

localization of Rab1 and actin filaments in association with tubulovesicular membranes, Rab1 is presumably more effective at impeding WHAMM-mediated actin assembly at the vesicle head than along the length of the tubule. Thus the engagement of WHAMM by a combination of positive and negative regulators would provide an appropriate level of actin assembly for coordinating the tubulovesicular membrane remodeling process. Of interest, our results with

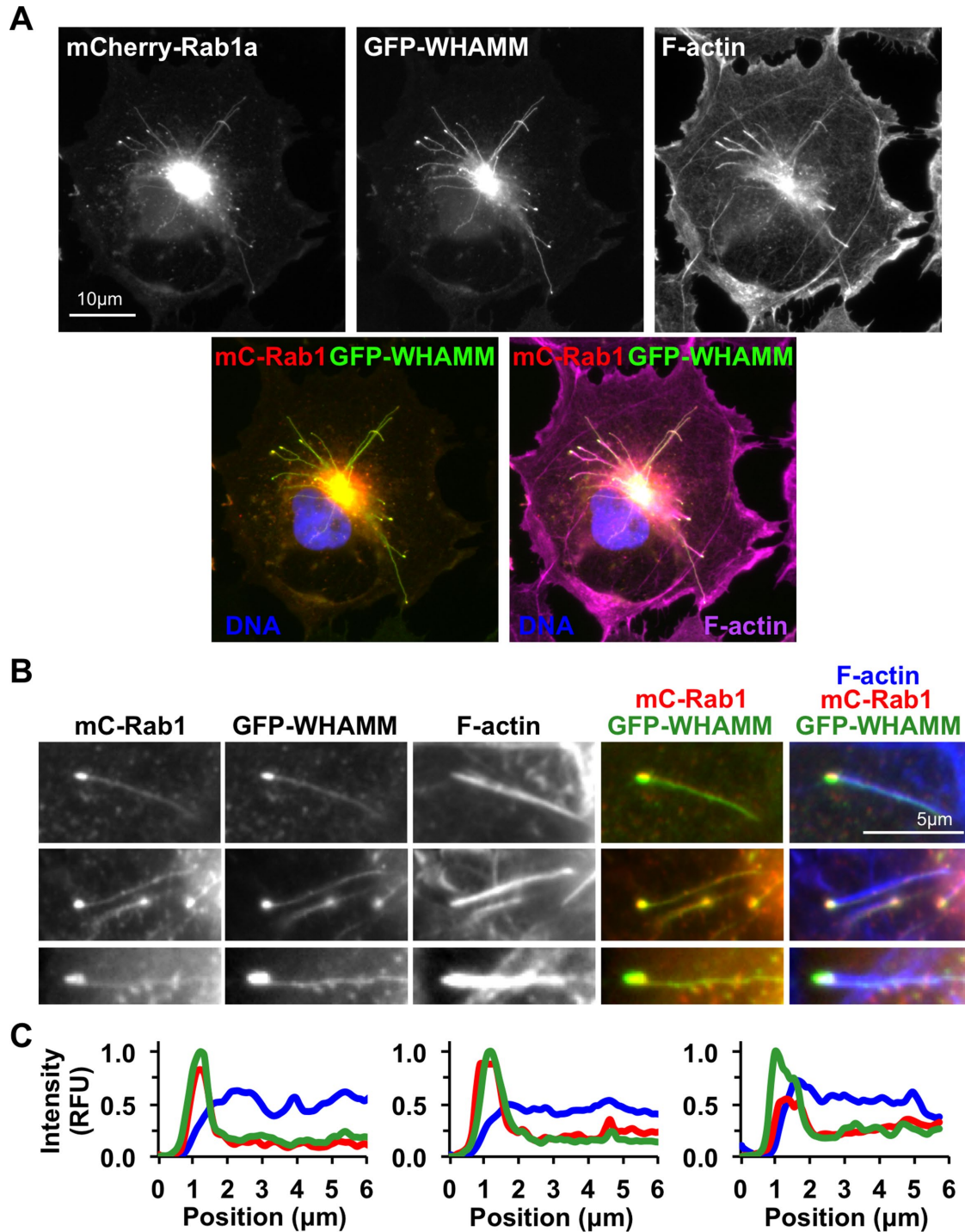


**FIGURE 7:** Actin assembly is limited around the heads of tubulovesicular structures. (A) Cos7 cells coexpressing mCherry-Rab1a and GFP-WHAMM were fixed and stained with phalloidin to label actin filaments and DAPI to visualize DNA (Supplemental Figure S4). (B) Colocalization of Rab1 with WHAMM and the position of actin filaments in association with tubulovesicular membranes are highlighted in magnified images. (C) Relative fluorescence intensity of GFP-WHAMM (green), mCherry-Rab1a (red), and F-actin (blue) along the length of three representative tubulovesicular structures. For normalization purposes, the maximum intensity of WHAMM fluorescence was set to 1 relative fluorescence unit (RFU) on the y-axis and 1  $\mu\text{m}$  on the x-axis.

Rab1 parallel those with microtubules, in that microtubules are important for membrane tubulation in cells (Campellone *et al.*, 2008) and inhibit actin assembly by recombinant WHAMM *in vitro* (Shen *et al.*, 2012). Molecules that stimulate WHAMM-associated actin nucleation have not yet been uncovered, and it is also not known

whether WHAMM exists in a multisubunit regulatory complex similar to the WAVE and WASH proteins. Thus determining the identities of other WHAMM-interacting factors and deciphering how WHAMM and additional WASP-family proteins are controlled by their binding partners are important goals for the future.

## MATERIALS AND METHODS

### Plasmids, bacmids, and viruses

Plasmids, bacmids, and baculoviruses encoding human WHAMM were described previously (Campellone *et al.*, 2008; Shen *et al.*, 2012). Plasmids encoding fluorescent versions of canine Rab1a, which is identical to human Rab1a, were generated by PCR using a GFP-Rab1a template (a gift from Craig Roy, Yale University, New Haven, CT) and cloned as a KpnI-NotI fragment into pKC-EGFP-C1 and pKC-mCherry-C1 (Campellone *et al.*, 2008). The GST-RhoD plasmid (a gift from Pontus Aspenstrom, Karolinska Institutet, Stockholm, Sweden) was described previously (Gad *et al.*, 2012). Fluorescent versions of murine RhoD were constructed by subcloning RhoD as a BamHI-EcoRI fragment into pKC-EGFP-C1 and pKC-mCherry-C1. Other G-proteins were also expressed using pKC-EGFP-C1. To generate a plasmid for expression of GST-Rab1a in *E. coli*, Rab1a was cloned into the BamHI site of pGEX-4T-1 (GE Healthcare, Pittsburgh, PA). To create a baculovirus expression construct, GST-Rab1a was cloned into the KpnI-NotI sites of pKC-FastBacHTA (Campellone *et al.*, 2008). GST-Rab5a was generated similarly by subcloning murine Rab5a from an mCherry-Rab5a template (27679; Addgene, Cambridge, MA) as an EcoRI-NotI fragment into pKC-FastBacHTA. Recombinant baculoviruses were generated using the Bac-to-Bac system (Invitrogen, Carlsbad, CA; Campellone *et al.*, 2008).

### Bacterial and eukaryotic cell culture

All bacteria were cultured in Luria-Bertani medium with appropriate antibiotics at 37°C. Plasmids were maintained in *E. coli* XL-1 Blue (Stratagene, San Diego, CA) and purified using standard miniprep kits (Machery-Nagel, Bethlehem, PA) before transfection. During bacterial expression, GST-fusion proteins were produced in *E. coli* Rosetta(DE3)pLysS (EMD Millipore, Billerica, MA). *Sf9* insect cells were grown in ESF921 medium (Expression Systems, Davis, CA) at 28°C and infected with baculoviruses encoding MBP- or GST-fusion proteins at a multiplicity of infection of ~1. Cos7, HeLa, and HFF cells were cultured in DMEM plus 10% fetal bovine serum and antibiotic-antimycotic (Invitrogen) at 37°C in 5% CO<sub>2</sub>. Transfections with DNA or RNA used Lipofectamine-LTX or RNAiMAX (Invitrogen), respectively (Campellone *et al.*, 2008). Control siRNAs, siRNAs to glyceraldehyde-3-phosphate dehydrogenase, and siRNA pair #3 to Rab1a+b were from Ambion, and siRNA pairs #1 and 2 to Rab1a+b and siRNAs #1 and 2 to RhoD were from Sigma-Aldrich (St. Louis, MO). For selection of HFF clones stably transfected with LAP or LAP-WHAMM, media were supplemented with 750 µg/ml G418. To induce LAP expression, 7.6 mM sodium butyrate was added for 12–18 h.

### Fluorescence microscopy

For most analyses, cells grown on glass coverslips were fixed using 2.5% paraformaldehyde and permeabilized with 0.1% Triton X-100 in phosphate-buffered saline (PBS). To visualize endogenous Rab1 or GM130, cells were treated with rabbit anti-Rab1b (Santa Cruz Biotechnology, Dallas, TX) or mouse anti-GM130 (BD Biosciences, San Jose, CA) primary antibodies and Alexa 488-, 555-, 568-, or 647-conjugated secondary antibodies (Invitrogen). F-actin was detected using 4 U/ml Alexa-conjugated phalloidin (Invitrogen), and DNA was labeled using 1 µg/ml 4',6-diamidino-2-phenylindole (DAPI; Invitrogen). These fixation and staining conditions are incompatible with the methanol treatment required to immunostain for WHAMM (Campellone *et al.*, 2008). Coverslips were mounted in ProLong Gold antifade (Invitrogen), and images were captured using 60×/1.40 numerical aperture (NA) or 100×/1.45 NA PlanApo

objective lenses on a Nikon Ti-E microscope equipped with an Andor Clara-E camera. For live cells, images were acquired at 1- to 10-s intervals, converted to 16-bit format, and processed using ImageJ software (National Institutes of Health, Bethesda, MD).

### Microscopic quantification

For measuring membrane tubulation, cells expressing GFP/mCherry-tagged WHAMM and/or Rab1a were scored positive for tubulation if WHAMM fluorescence appeared in tubular structures that were >1 µm or >5 µm in length and not within the juxtannuclear Golgi. To avoid the microtubule bundling that arises from WHAMM overexpression (Campellone *et al.*, 2008), Cos7 cells grown in six-well plates were transfected with only 35–75 ng of WHAMM plasmids per well. Microscopic quantification was performed in a blinded manner by coding coverslips and scoring randomly chosen cells. Fluorescence intensity line scans were generated using the histogram analysis tool in ImageJ. Statistical significance and *p* values were evaluated using analysis of variance (ANOVA), Mann-Whitney, Dunnett, and *t* tests in the GraphPad Prism software package.

### SDS-PAGE and immunoblotting

To prepare cytoplasmic extracts, transfected cells were collected in PBS plus 2 mM EDTA and lysed in 50 mM Tris, pH 7.6, 50 mM NaCl, 1% Triton X-100, 1 mM phenylmethylsulfonyl fluoride, and 10 µg/ml each of aprotinin, leupeptin, pepstatin, and chymostatin (Sigma-Aldrich) before mixing with SDS-PAGE sample buffer. For fractionation, cells were lysed in 10 mM Tris pH 7.6, 250 mM sucrose, and 1 mM EDTA plus inhibitors by passage through a 27-gauge needle and centrifuged at 16,000 × *g* to remove nuclei and debris. Clarified lysates were then centrifuged at 54,000 rpm in a TLA100 rotor (Beckman, Brea, CA) for 76 min, and the resulting pellet (membrane) and supernatant (cytosol) were mixed with sample buffer to equivalent volumes. All samples were boiled and analyzed by SDS-PAGE and Coomassie blue staining or transferred to nitrocellulose filters and stained with Ponceau S. Filters were probed with chicken anti-WHAMM or rabbit anti-GFP (Campellone *et al.*, 2008), rabbit anti-N-WASP (Rohatgi *et al.*, 1999), rabbit anti-Rab1b or mouse anti-RhoD (Santa Cruz Biotechnology), or mouse anti-tubulin (Developmental Studies Hybridoma Bank, Iowa City, IA) antibodies. After treatment with horseradish peroxidase-conjugated secondary antibodies, bands were visualized using enhanced chemiluminescence (GE Healthcare). Densitometry was performed in ImageJ by measuring the mean pixel intensity of protein-specific bands and normalizing those values to background staining.

### Protein purification and analysis

Bacteria expressing GST-Rab1a derivatives or GST-RhoD were collected by centrifugation, resuspended in PBS plus 200 mM KCl, 5% glycerol, and inhibitors, and frozen in liquid nitrogen. Thawed suspensions were lysed by sonication in the presence of 1 mg/ml lysozyme. GST fusions were isolated via glutathione affinity beads (GE Healthcare) and eluted in 50 mM Tris, pH 8.0, 200 mM KCl, and 10 mM glutathione (Campellone *et al.*, 2008). For some experiments, GST-RhoD eluates were supplemented with 75 µM GTPγS. Baculovirus-infected *Sf9* cells expressing MBP-WHAMM derivatives were collected by centrifugation, resuspended in 20 mM Tris, pH 7.6, 250 mM NaCl, 100 mM KCl, 1 mM dithiothreitol (DTT), 1 mM EDTA, 5% glycerol, and inhibitors, and frozen in liquid nitrogen. Suspensions were freeze-thawed, treated with 0.02% NP-40, sonicated using a Fisher dismembrator, and centrifuged for 20 min at 35,000 rpm at 4°C in a 70.1Ti rotor (Beckman). To purify the MBP-fusion proteins, 0.45-µm-filtered supernatants were mixed with

amylose resin (New England Biolabs, Ipswich, MA), and bound proteins were collected in 20 mM Tris, pH 7.6, 250 mM NaCl, 100 mM KCl, 1 mM DTT, 1 mM EDTA, 5% glycerol, and 10 mM maltose (Shen *et al.*, 2012). MBP-fusions were dialyzed into 20 mM 3-(*N*-morpholino)propanesulfonic acid (pH 7.0), 100 mM KCl, 2 mM MgCl<sub>2</sub>, 5 mM ethylene glycol tetraacetic acid, 1 mM EDTA, and 10% glycerol before use in pyrene-actin assembly assays. *Sf9* cells expressing GST-Rab1a or GST-Rab5a were collected by centrifugation, washed with PBS, resuspended in PBS plus 125 mM NaCl, 100 mM KCl, 1 mM MgCl<sub>2</sub>, 5% glycerol, 0.2 mM GTP, and inhibitors, and frozen in liquid nitrogen. After two freeze–thaw cycles, suspensions were sonicated and passed through a 22-gauge needle. Debris was pelleted by centrifugation for 35 min at 10,000 rpm at 4°C in a SS34 rotor (Sorvall, Waltham, MA), and the supernatant was resonicated twice and passed through a 0.45-μm filter to generate cytoplasmic extract. Membranes and cytosol were then separated by centrifugation for 54 min at 44,000 rpm at 4°C in a 60Ti rotor (Beckman). The membrane fraction was washed once with buffer, repelleted, resuspended in buffer containing 0.6% 3-[(3-cholamidopropyl)dimethylammonio]-1-propanesulfonate (CHAPS), and again pelleted to yield a supernatant containing extracted membrane proteins, similar to published methods (Nuoffer *et al.*, 1995). To purify the cytosolic or membrane-extracted forms of Rab1—GST-Rab1(C) and GST-Rab1(M), respectively—each sample was mixed with glutathione affinity beads, and proteins were eluted in 50 mM Tris, pH 8.0, containing 200 mM KCl, 10 mM glutathione, and 0.1% CHAPS. GST-Rab5(M) was isolated in a similar manner to GST-Rab1(M). All protein quantities were measured using Bradford assays (Bio-Rad, Hercules, CA), and purities were confirmed by SDS–PAGE analyses. Aliquots were frozen in liquid nitrogen and stored at –80°C.

### Pull-down assays

For GST pull downs, GST-fusion proteins purified from bacteria were immobilized on glutathione-agarose beads and mixed with Cos7 cell extracts at 23°C for 1 h in GST buffer. After 2300-rpm centrifugation steps and washing, bead-associated proteins were eluted by boiling in sample buffer. For MBP pull downs, MBP, MBP-WHAMM, and MBP-WMD were immobilized on amylose-agarose beads and mixed with 3.3 μM purified GST, GST-Rab1(C), or GST-Rab1(M) at 23°C for 1 h in MBP freezing buffer supplemented with 20 μM GTP. After centrifugation and washing, bead-associated proteins were eluted by boiling in sample buffer.

### Pyrene-actin assembly assays

Assembly assays were performed essentially as described previously (Campellone *et al.*, 2008). Briefly, 2 μM actin (7% pyrene labeled) was polymerized in the presence of 20 nM Arp2/3 complex with or without its regulators. Maximal actin assembly rates were calculated by measuring the slopes of polymerization curves at half of the maximal F-actin concentration.

### ACKNOWLEDGMENTS

We thank David Stephens, Craig Roy, and Pontus Aspenstrom for reagents and Sarah Grout for assistance with pyrene assays. K.G.C. was supported by a Leukemia and Lymphoma Society Career Development Fellowship, a University of Connecticut Research Foundation Grant, an American Heart Association Scientist Development Grant, and National Institutes of Health Grant R01 GM107441. A.J.R. and S.H. were supported by University of Connecticut student fellowships. M.D.W. was supported by National Institutes of Health Grant R01 GM059609.

### REFERENCES

- Allan BB, Moyer BD, Balch WE (2000). Rab1 recruitment of p115 into a cis-SNARE complex: programming budding COPII vesicles for fusion. *Science* 289, 444–448.
- Alvarez C, Garcia-Mata R, Brandon E, Sztul E (2003). COPI recruitment is modulated by a Rab1b-dependent mechanism. *Mol Biol Cell* 14, 2116–2127.
- Aspenstrom P (2014). Atypical Rho GTPases RhoD and Rif integrate cytoskeletal dynamics and membrane trafficking. *Biol Chem* 395, 477–484.
- Blom M, Reis K, Nehru V, Blom H, Gad AK, Aspenstrom P (2015). RhoD is a Golgi component with a role in anterograde protein transport from the ER to the plasma membrane. *Exp Cell Res* 333, 208–219.
- Brandon E, Szul T, Alvarez C, Grabski R, Benjamin R, Kawai R, Sztul E (2006). On and off membrane dynamics of the endoplasmic reticulum-golgi tethering factor p115 in vivo. *Mol Biol Cell* 17, 2996–3008.
- Campellone KG, Webb NJ, Znameroski EA, Welch MD (2008). WHAMM is an Arp2/3 complex activator that binds microtubules and functions in ER to Golgi transport. *Cell* 134, 148–161.
- Campellone KG, Welch MD (2010). A nucleator arms race: cellular control of actin assembly. *Nat Rev Mol Cell Biol* 11, 237–251.
- Cheeseman IM, Desai A (2005). A combined approach for the localization and tandem affinity purification of protein complexes from metazoans. *Sci STKE* 2005, pl1.
- Chen Z, Borek D, Padrick SB, Gomez TS, Metlagel Z, Ismail AM, Umetani J, Billadeau DD, Otwinowski Z, Rosen MK (2010). Structure and control of the actin regulatory WAVE complex. *Nature* 468, 533–538.
- Coutts AS, La Thangue NB (2015). Actin nucleation by WH2 domains at the autophagosome. *Nat Commun* 6, 7888.
- Coutts AS, Weston L, La Thangue NB (2009). A transcription co-factor integrates cell adhesion and motility with the p53 response. *Proc Natl Acad Sci USA* 106, 19872–19877.
- Dang I, Gorelik R, Sousa-Blin C, Derivery E, Guerin C, Linkner J, Nemethova M, Dumortier JG, Giger FA, Chipysheva TA, *et al.* (2013). Inhibitory signalling to the Arp2/3 complex steers cell migration. *Nature* 503, 281–284.
- Eden S, Rohatgi R, Podtelejnikov AV, Mann M, Kirschner MW (2002). Mechanism of regulation of WAVE1-induced actin nucleation by Rac1 and Nck. *Nature* 418, 790–793.
- Egea G, Serra-Peinado C, Salcedo-Sicilia L, Gutierrez-Martinez E (2013). Actin acting at the Golgi. *Histochem Cell Biol* 140, 347–360.
- Gad AK, Nehru V, Ruusala A, Aspenstrom P (2012). RhoD regulates cytoskeletal dynamics via the actin nucleation-promoting factor WASp homologue associated with actin Golgi membranes and microtubules. *Mol Biol Cell* 23, 4807–4819.
- Gillingham AK, Munro S (2007). The small G proteins of the Arf family and their regulators. *Annu Rev Cell Dev Biol* 23, 579–611.
- Hehny H, Stames M (2007). Regulating cytoskeleton-based vesicle motility. *FEBS Lett* 581, 2112–2118.
- Hutagalung AH, Novick PJ (2011). Role of Rab GTPases in membrane traffic and cell physiology. *Physiol Rev* 91, 119–149.
- Innocenti M, Gerboth S, Rottner K, Lai FP, Hertzog M, Stradal TE, Frittoli E, Didry D, Polo S, Disanza A, *et al.* (2005). Abi1 regulates the activity of N-WASP and WAVE in distinct actin-based processes. *Nat Cell Biol* 7, 969–976.
- Kahn RA (2009). Toward a model for Arf GTPases as regulators of traffic at the Golgi. *FEBS Lett* 583, 3872–3879.
- Kast DJ, Zajac AL, Holzbaur EL, Ostap EM, Dominguez R (2015). WHAMM directs the Arp2/3 complex to the ER for autophagosome biogenesis through an actin comet tail mechanism. *Curr Biol* 25, 1791–1797.
- Kim AS, Kakalis LT, Abdul-Manan N, Liu GA, Rosen MK (2000). Autoinhibition and activation mechanisms of the Wiskott-Aldrich syndrome protein. *Nature* 404, 151–158.
- Koronakis V, Hume PJ, Humphreys D, Liu T, Horning O, Jensen ON, McGhie EJ (2011). WAVE regulatory complex activation by cooperating GTPases Arf and Rac1. *Proc Natl Acad Sci USA* 108, 14449–14454.
- Luna A, Matas OB, Martinez-Menarguez JA, Mato E, Duran JM, Ballesta J, Way M, Egea G (2002). Regulation of protein transport from the Golgi complex to the endoplasmic reticulum by CDC42 and N-WASP. *Mol Biol Cell* 13, 866–879.
- Marie M, Dale HA, Sannerud R, Saraste J (2009). The function of the intermediate compartment in pre-Golgi trafficking involves its stable connection with the centrosome. *Mol Biol Cell* 20, 4458–4470.
- Matas OB, Martinez-Menarguez JA, Egea G (2004). Association of Cdc42/N-WASP/Arp2/3 signaling pathway with Golgi membranes. *Traffic* 5, 838–846.

- Miki H, Sasaki T, Takai Y, Takenawa T (1998a). Induction of filopodium formation by a WASP-related actin-depolymerizing protein N-WASP. *Nature* 391, 93–96.
- Miki H, Suetsugu S, Takenawa T (1998b). WAVE, a novel WASP-family protein involved in actin reorganization induced by Rac. *EMBO J* 17, 6932–6941.
- Mizuno-Yamasaki E, Rivera-Molina F, Novick P (2012). GTPase networks in membrane traffic. *Annu Rev Biochem* 81, 637–659.
- Monetta P, Slavin I, Romero N, Alvarez C (2007). Rab1b interacts with GBF1 and modulates both ARF1 dynamics and COPI association. *Mol Biol Cell* 18, 2400–2410.
- Moyer BD, Allan BB, Balch WE (2001). Rab1 interaction with a GM130 effector complex regulates COPII vesicle cis-Golgi tethering. *Traffic* 2, 268–276.
- Nuoffer C, Peter F, Balch WE (1995). Purification of His6-tagged Rab1 proteins using bacterial and insect cell expression systems. *Methods Enzymol* 257, 3–9.
- Peter F, Nuoffer C, Pind SN, Balch WE (1994). Guanine nucleotide dissociation inhibitor is essential for Rab1 function in budding from the endoplasmic reticulum and transport through the Golgi stack. *J Cell Biol* 126, 1393–1406.
- Pind SN, Nuoffer C, McCaffery JM, Plutner H, Davidson HW, Farquhar MG, Balch WE (1994). Rab1 and Ca<sup>2+</sup> are required for the fusion of carrier vesicles mediating endoplasmic reticulum to Golgi transport. *J Cell Biol* 125, 239–252.
- Plutner H, Cox AD, Pind S, Khosravi-Far R, Bourne JR, Schwaninger R, Der CJ, Balch WE (1991). Rab1b regulates vesicular transport between the endoplasmic reticulum and successive Golgi compartments. *J Cell Biol* 115, 31–43.
- Pollard TD, Cooper JA (2009). Actin, a central player in cell shape and movement. *Science* 326, 1208–1212.
- Prehoda KE, Scott JA, Mullins RD, Lim WA (2000). Integration of multiple signals through cooperative regulation of the N-WASP-Arp2/3 complex. *Science* 290, 801–806.
- Rohatgi R, Ma L, Miki H, Lopez M, Kirchhausen T, Takenawa T, Kirschner MW (1999). The interaction between N-WASP and the Arp2/3 complex links Cdc42-dependent signals to actin assembly. *Cell* 97, 221–231.
- Rotty JD, Wu C, Bear JE (2013). New insights into the regulation and cellular functions of the ARP2/3 complex. *Nat Rev Mol Cell Biol* 14, 7–12.
- Sannerud R, Marie M, Nizak C, Dale HA, Pernet-Gallay K, Perez F, Goud B, Saraste J (2006). Rab1 defines a novel pathway connecting the pre-Golgi intermediate compartment with the cell periphery. *Mol Biol Cell* 17, 1514–1526.
- Saraste J, Dale HA, Bazzocco S, Marie M (2009). Emerging new roles of the pre-Golgi intermediate compartment in biosynthetic-secretory trafficking. *FEBS Lett* 583, 3804–3810.
- Saraste J, Lahtinen U, Goud B (1995). Localization of the small GTP-binding protein rab1p to early compartments of the secretory pathway. *J Cell Sci* 108, 1541–1552.
- Satoh A, Wang Y, Malsam J, Beard MB, Warren G (2003). Golgin-84 is a rab1 binding partner involved in Golgi structure. *Traffic* 4, 153–161.
- Schluter K, Waschbusch D, Anft M, Hugging D, Kind S, Hanisch J, Lakisic G, Gautreau A, Barnekow A, Stradal TE (2014). JMY is involved in anterograde vesicle trafficking from the trans-Golgi network. *Eur J Cell Biol* 93, 194–204.
- Seaman MN, Gautreau A, Billadeau DD (2013). Retromer-mediated endosomal protein sorting: all WASHed up! *Trends Cell Biol* 23, 522–528.
- Shen QT, Hsiue PP, Sindelar CV, Welch MD, Campellone KG, Wang HW (2012). Structural insights into WHAMM-mediated cytoskeletal coordination during membrane remodeling. *J Cell Biol* 199, 111–124.
- Slavin I, Garcia IA, Monetta P, Martinez H, Romero N, Alvarez C (2011). Role of Rab1b in COPII dynamics and function. *Eur J Cell Biol* 90, 301–311.
- Steffen A, Rottner K, Ehinger J, Innocenti M, Scita G, Wehland J, Stradal TE (2004). Sra-1 and Nap1 link Rac to actin assembly driving lamellipodia formation. *EMBO J* 23, 749–759.
- Tisdale EJ, Bourne JR, Khosravi-Far R, Der CJ, Balch WE (1992). GTP-binding mutants of rab1 and rab2 are potent inhibitors of vesicular transport from the endoplasmic reticulum to the Golgi complex. *J Cell Biol* 119, 749–761.
- Wagner AR, Luan Q, Liu SL, Nolen BJ (2013). Dip1 defines a class of Arp2/3 complex activators that function without preformed actin filaments. *Curr Biol* 23, 1990–1998.
- Zanetti G, Pahuja KB, Studer S, Shim S, Schekman R (2011). COPII and the regulation of protein sorting in mammals. *Nat Cell Biol* 14, 20–28.
- Zuchero JB, Coutts AS, Quinlan ME, Thangue NB, Mullins RD (2009). p53-cofactor JMY is a multifunctional actin nucleation factor. *Nat Cell Biol* 11, 451–459.